

Symmetrized partial-wave method for density-functional cluster calculations

F. W. Averill* and Gayle S. Painter

Oak Ridge National Laboratory, Oak Ridge, Tennessee 37831-6114

(Received 16 May 1994)

The computational advantage and accuracy of the Harris method is linked to the simplicity and adequacy of the reference-density model. In an earlier paper, we investigated one way the Harris functional could be extended to systems outside the limits of weakly interacting atoms by making the charge density of the interacting atoms self-consistent within the constraints of overlapping spherical atomic densities. In the present study, a method is presented for augmenting the interacting atom charge densities with symmetrized partial-wave expansions on each atomic site. The added variational freedom of the partial waves leads to a scheme capable of giving exact results within a given exchange-correlation approximation while maintaining many of the desirable convergence and stability properties of the original Harris method. Incorporation of the symmetry of the cluster in the partial-wave construction further reduces the level of computational effort. This partial-wave cluster method is illustrated by its application to the dimer C_2 , the hypothetical atomic cluster Fe_6Al_8 , and the benzene molecule.

I. INTRODUCTION

The first-principles calculation of the electronic structure, geometries, and relative energetics of atomic clusters and molecules of ever increasing size has been made possible by rapid advances in computer technology and the development of high performance codes. Much of this success has been achieved with implementations of the local-density approximation (LDA) to the density-functional theory of Hohenberg, Kohn, and Sham.¹ In all of the self-consistent-field (SCF) versions of this method, the computationally intensive step is solving the Poisson equation for the electronic charge density calculated at each iteration. Although a number of accurate approaches to this problem have been developed, the search for simpler and more numerically efficient methods has continued. The availability of massively parallel-processing computers has heightened interest in numerical methods which can use this computer architecture to advantage.

One popular strategy to solving the Poisson equation is to approximate the true electronic charge density of the system by a superposition of atom-centered functions for which Coulomb potentials are easily evaluated. The Coulomb potential of the entire molecular density is then simply a sum of the atom-centered potentials. Over the years, many techniques²⁻⁷ have been found for choosing sets of functions for carrying out this density-fitting procedure. Often the first step is to superimpose the spherically averaged densities of the constituent atoms of the cluster. In some approximations, the occupation numbers of the atomic orbitals in the molecular environment are allowed to vary in some sort of self-consistent way. This is the basis of the self-consistent atom fragment (SCAF) method.⁸ As expected, this approximation is most appropriate in systems where the atoms interact only weakly, but it is often satisfactory in ionic systems as well. However, this representation in terms of superimposed spherically averaged atom densities does not usual-

ly provide the angular dependence necessary to describe covalent bond densities. In such cases, the atom fit densities must be supplemented by additional atom- or bond-centered functions whose derivation, in the past, has not always been obvious.

These early density-fitting methods displayed rather slow convergence properties, and instabilities in the energies calculated from them. However, these problems were largely overcome in the variational fitting procedure of Dunlap, Connolly, and Sabin (DCS).⁵ In their procedure the electron self-interaction energy $E_{ee}[\rho]$ is expanded in terms of the difference density $\tilde{\Delta}\rho = \rho - \tilde{\rho}$, giving

$$E_{ee}[\rho] = E_{ee}[\tilde{\rho}] + \int \tilde{\Delta}\rho(\mathbf{r})\tilde{\varphi}(\mathbf{r})d\mathbf{r} + E_{ee}[\tilde{\Delta}\rho], \quad (1)$$

where ρ is the true molecular density, $\tilde{\rho}$ is the approximate fit to that density, and $\tilde{\varphi}(\mathbf{r})$ is the Coulomb potential of $\tilde{\rho}$. The electron repulsion energy $E_{ee}[\rho]$ is then approximated by omitting the difference density self-interaction, i.e.,

$$E_{ee}[\rho] \approx E_{ee}[\tilde{\rho}] + \int \tilde{\Delta}\rho(\mathbf{r})\tilde{\varphi}(\mathbf{r})d\mathbf{r}, \quad (2)$$

where the fit density $\tilde{\rho}$ is chosen to minimize $E_{ee}[\tilde{\Delta}\rho]$ within the space of the fit basis set.

In more recent work, Averill and Painter⁸ have shown that the attractive convergence properties of the DCS method can be modestly improved by also expanding the exchange-correlation energy $E_{xc}[\tilde{\rho}]$ in terms of the difference density, so that

$$E_{xc}[\rho] \approx E_{xc}[\tilde{\rho}] + \int \tilde{\Delta}\rho(\mathbf{r})\tilde{\mu}_{xc}(\mathbf{r})d\mathbf{r}, \quad (3)$$

where $\tilde{\mu}_{xc}(\mathbf{r})$ is the single-electron exchange-correlation potential due to $\tilde{\rho}$. When approximate forms for $E_{ee}[\rho]$ and $E_{xc}[\tilde{\rho}]$ are used as in Eqs. (2) and (3), the resulting total-energy expression

$$E_H = \sum_i n_i \epsilon_i - \int \bar{\rho}(\mathbf{r}) \left[\frac{1}{2} \bar{\phi}(\mathbf{r}) + \bar{\mu}_{xc}(\mathbf{r}) \right] d\mathbf{r} + E_{xc}[\bar{\rho}] + E_{NN}, \quad (4)$$

is equivalent to that developed in different contexts by Harris,⁹ Foulkes and Haydock,¹⁰ and Delley *et al.*¹¹ The one-electron energies $\{\epsilon_i\}$ and the associated molecular-orbital occupation numbers $\{n_i\}$ are found by solving the one-electron self-consistency equation

$$\left[-\frac{1}{2} \nabla^2 + \bar{\phi}(\mathbf{r}) + V_N(\mathbf{r}) + \bar{\mu}_{xc}(\mathbf{r}) \right] \Psi_i(\mathbf{r}) = \epsilon_i \Psi_i(\mathbf{r}). \quad (5)$$

In earlier work,⁸ we showed that in some systems the frozen-atom-fragment (FAF) approximation of Harris could be improved upon by fitting the molecular density with spherically averaged atomic densities whose valence shell "occupation numbers" are allowed to vary in a self-consistent way, the self-consistent-atom-fragment (SCAF) method. In the present work we present a method in Sec. II for systematically improving the completeness of this density fit basis by the addition of atom-centered symmetrized partial waves. This latest adaptation of the Harris formalism will be referred to as the self-consistent partial-wave (SCPW) method. Our application of partial waves in the SCPW method is very similar to that described by Delley⁷ and Becke,¹² but differs in details which will be discussed in Sec. IV.

Section III illustrates application of the SCPW method to a variety of clusters with differing bond characteristics. The first case is the well-studied diatomic molecule C_2 , which displayed the largest error in our earlier SCAF calculations.⁸ We also present results for the hypothetical atomic cluster Fe_6Al_8 , which demonstrates the accuracy provided by the SCAF method alone. Finally, the strongly covalent benzene molecule was studied to assess the partial-wave convergence rate.

II. SELF-CONSISTENT PARTIAL-WAVE METHOD

In this section we provide details of the charge-density decomposition, symmetrization of the partial-wave basis, and a numerical integration method for general as well as symmetry-adapted calculations.

A. Partial-wave projections of the charge density

As a first step in the decomposition of the cluster charge density into a sum of atom-centered functions, we subtract from the molecular density (generated from the eigenfunctions at some stage of iteration) the spherically averaged density ρ_j of each of the constituent atoms. This defines a difference density

$$\Delta\rho(\mathbf{r}) = \rho(\mathbf{r}) - \sum_j \rho_j(r), \quad (6)$$

where the sum is over the N atoms of the cluster. The way in which the occupation numbers of the valence atomic orbitals defining ρ_j are chosen is not critical to the method. One choice is simply to let them assume the nominal values of the isolated atoms. For ionic systems,

it is useful to choose the occupation numbers from a SCAF calculation.

The next step is to rewrite the difference density as a sum of atom centered functions P_j ,

$$\Delta\rho(\mathbf{r}) = \sum_j P_j(\mathbf{r}). \quad (7)$$

This is most easily accomplished by projection techniques pioneered by Boys and Rajagopal¹³ and further refined by Becke¹⁴ and Delley.⁷ In our case, P_j is defined by a set of atom-centered weight functions ω_j such that

$$P_j(\mathbf{r}) = \omega_j(\mathbf{r}) \Delta\rho(\mathbf{r}), \quad (8)$$

and

$$\sum_j \omega_j(\mathbf{r}) = 1. \quad (9)$$

On examining several different forms of the weight function ω_j , we have found the homonuclear fuzzy-cell function of Becke¹⁴ to be the most satisfactory. The details for generating this function are found in Ref. 14, but the distinctive characteristics of Becke's ω_j are (1) ω_j approaches unity for points \mathbf{r} well inside the Voronoi polyhedron centered on site j ; (2) ω_j smoothly approaches zero as \mathbf{r} moves into the proximity of and outside the cell boundary; and (3) ω_j is identically zero at the center of sites other than j . This projection function when applied to $\Delta\rho(\mathbf{r})$ [Eq. (8)] has the desirable effect of producing a function P_j which is large in magnitude near site j and which approaches zero away from site j . Carrying out partial-wave projections about each site j ,

$$\rho_{lm}^j(r) = \int_{\Omega} Y_{lm}^j(\hat{r}) P_j(\mathbf{r}) d\Omega \quad (10)$$

determines the approximate representation of P_j ,

$$P_j(\mathbf{r}) \approx \sum_{l=0}^{l_{\max}(j)} \sum_{m=-l}^{+l} \rho_{lm}^j(r) Y_{lm}^j(\hat{r}), \quad (11)$$

with accuracy controlled by the cutoff l value [$l_{\max}(j)$]. It has been our experience that the Harris total-energy functional [Eq. (4)] converges to the same tolerance as the standard Kohn-Sham expression with roughly half as many l values. Since the total number of partial waves in Eq. (11) goes as $[l_{\max}(j)+1]^2$, use of the Harris functional provides an appreciable savings in computational effort. The number of partial-wave terms can usually be further reduced by symmetry considerations, as will be discussed in Sec. II B.

Finally, putting all the pieces together, we can write the total approximate density $\bar{\rho}(\mathbf{r})$ as a sum of atom-centered functions:

$$\bar{\rho}(\mathbf{r}) = \sum_j f_j(\mathbf{r}), \quad (12)$$

where

$$f_j(\mathbf{r}) = \rho_j(r) + \sum_{l=0}^{l_{\max}(j)} \sum_{m=-l}^{+l} \rho_{lm}^j(r) Y_{lm}^j(\hat{r}). \quad (13)$$

The density $\bar{\rho}(\mathbf{r})$ is designated as an approximate one to reflect the truncation in the l expansion of Eq. (13).

The Coulomb potential $\bar{\varphi}(\mathbf{r})$ associated with $\bar{\rho}(\mathbf{r})$ is then calculated as

$$\bar{\varphi}(\mathbf{r}) = \sum_j g_j(\mathbf{r}), \quad (14)$$

where

$$g_j(\mathbf{r}) = v_j(r) + \sum_{l=0}^{l_{\max}(j)} \sum_{m=-l}^{+l} v_{lm}^j(r) Y_{lm}^j(\hat{r}). \quad (15)$$

The potential $v_j(r)$ associated with $\rho_j(r)$ and the potential $v_{lm}^j(r)$ corresponding to $\rho_{lm}^j(r)$ are the radial partial-wave projections centered at site j . These functions are evaluated numerically using efficient well-known algorithms.¹⁵

Among the advantages of the scheme represented by Eqs. (12)–(15) is the high degree of flexibility it provides. Ignoring the partial-wave terms altogether, either the FAF approximation or the SCAF approximation can be recovered. As $l_{\max}(j)$ is increased in the full SCPW implementation, the calculation becomes more complete. Also, the different site expansions in l values of Eqs. (13) and (15) allow the numerical effort to be focused on those cluster atoms in a specific application where the chemical interest is often localized. Notice also that the only approximation in Eqs. (12)–(15) involves a projection of the difference density onto a set of partial waves. Consequently, the method does not require the independent development of a density fit basis as in other fitting methods.

The purpose of subtracting out the atom density $\rho_j(r)$ from the total density $\rho(\mathbf{r})$ in Eq. (6) is that this reduces much of the rapid radial dependence of $\rho(\mathbf{r})$, particularly that due to the core orbitals. This allows the use of a coarser radial point grid in solving for $\rho_{lm}^j(r)$ and $v_{lm}^j(r)$ near the nuclei than would otherwise be possible. Another attribute of this subtraction process is that it allows us to use the SCAF method as a starting point for a SCPW calculation. In those cases it can then be used as a good starting point in the self-consistency cycling in which partial wave densities are mixed.

B. Symmetrization of the partial waves and angular integration

The computational effort of evaluating the radial functions $\rho_{lm}^j(r)$ and $v_{lm}^j(r)$ can often be reduced considerably by making use of the symmetry properties of the cluster. Since the charge density $\rho(\mathbf{r})$ must transform like the totally symmetric A_1 representation under the rotation group of the cluster, only those $Y_{lm}(\hat{r})$'s on site j contributing to the linear combinations over sites transforming as A_1 are symmetry allowed in the partial-wave expansion of P_j . In some special cases, partial waves of a specific l value at site j will be forbidden by symmetry considerations. Most typically, for a given l value, there will be one or more linearly independent combinations of $Y_{lm}(\hat{r})$'s which transform as A_1 . Let

$$Y_L(\mathbf{r}) = c_1 y_1 + c_2 y_2 + \cdots + c_k y_k + \cdots + c_n y_n, \quad (16)$$

be one such contribution from site j , where y_k represents a $Y_{lm}(\hat{r})$ of fixed l with only m varying (we abbreviate the

l, m pair to L). The constants c_k can be determined to within a multiplicative constant by symmetry considerations alone. If there is more than one $Y_L(\mathbf{r})$ for a given l value, the c_k 's can be chosen to make those $Y_L(\mathbf{r})$'s orthogonal as well as linearly independent. The contribution of this linear combination to the partial wave projection of P_j is

$$h_L(\mathbf{r}) = I_L(r) Y_L(\hat{r}), \quad (17)$$

where $I_L(r)$ is a radial function centered at site j . The L expansion of Eq. (11) can then be rewritten as

$$P_j(\mathbf{r}) \approx \sum_L h_L(\mathbf{r}), \quad (18)$$

where the summation is over all linearly independent (and orthogonal) site j terms contributing to symmetrized combinations transforming like A_1 for l values up to $l_{\max}(j)$. Multiplying both sides of Eq. (18) by a particular $Y_L(\mathbf{r})$ and integrating over all angles about site j , it can be shown that

$$I_L(r) = \frac{\int_{\Omega} P_j(\mathbf{r}) Y_L(\hat{r}) d\Omega}{c_1^2 + c_2^2 + \cdots + c_n^2}. \quad (19)$$

Since both P_j and $Y_L(\mathbf{r})$ have the symmetry of site j , any reflection symmetry of the site can be used to reduce the limits of the integration in Eq. (19). Also, it is readily apparent that for a given l value, the radial functions $I_L(r)$ must be the same on all atom sites equivalent by symmetry to the j th site. The case of no symmetry is included in this scheme as simply another symmetry group.

C. Numerical integration

The angular integrations in Eq. (19) are performed numerically using product Gaussian formulas.¹⁶ Those numerical radial integrals necessary for energy evaluations are also performed with Gaussian quadrature. The number of Gaussian points needed in the angular integrations depends upon (1) the level of accuracy required for the calculation, (2) the reflection symmetry of the site, (3) the distance r from the site, (4) the $l_{\max}(j)$ value chosen for the site, and (5) the atomic number of the atoms involved.

The volume integrals that comprise the calculation of matrix elements and total energy could be evaluated using more efficient Voronoi polyhedral methods.^{17–19} For simplicity we have chosen the same fuzzy-cell method¹⁴ and point grid as used in the partial-wave projection. The SCPW computer code systematically partitions the volume around each inequivalent atom into spherical shells (and segments of shells) in order to minimize the number of Gaussian integration points. The program performs a limited search for optimal placement of the partitions and adjusts the number of Gaussian points within each partition in order to obtain a specified level of accuracy in the total charge integral. It has been our experience that an integration point distribution which accurately computes the total charge of the cluster will also achieve the accuracy necessary for the other numerical integrals. Even so, since Gaussian functions are used

in our basis set, many of the one-electron matrix elements are evaluated analytically without resorting to numerical methods. Only those integrals involving the exchange-correlation energy, the electron-electron Coulomb energy, and the partial-wave functions are evaluated numerically.

III. APPLICATIONS

In the following, we present results from SCPW calculations for three molecules chosen to illustrate the generality of the scheme as applied to different bonding situations. In Table I we summarize results for the binding energies of C_2 , Fe_6Al_8 , and C_6H_6 obtained by applying the SCPW method in seven different approximations for each system. In each calculation, a molecular-orbital basis set of double- ζ quality was obtained by the use of a full set of atomic orbitals, each written as a linear combination of Gaussian functions, supplemented by diffuse primitive Gaussian functions. The local-density approximation with the exchange-correlation functional of Vosko, Wilk, and Nusair^{20,21} was used in each case. In all SCAF calculations, a least-squares criterion was used in fitting the charge density.⁸ Binding energies were computed as the difference between the sum of total energies for atoms in their LDA ground-state configurations and the total energy of the cluster.

A. C_2

The experimental molecular ground-state configuration $^1\Sigma_g^+[1\pi_u(\uparrow\downarrow\downarrow)]$ was selected by choice of the one-electron occupation numbers. In the FAF calculation, the atom configuration was fixed at $C(2s^22p\uparrow^12p\downarrow^1)$. The interatomic separation was set at the computed equilibrium bond distance of 2.36 bohr. Inspecting the variation of the SCPW binding energy with respect to $l_{\max}(j)$ in Table I shows a quite striking rapid convergence. The $l_{\max}(j)=2$ results are accurate to almost 0.001 eV (about 0.01%). Even the $l_{\max}(j)=1$ results are sufficiently accurate for many purposes. Note that the error of the FAF energy relative to the SCPW result is almost 1.5 eV (20%), and the SCAF error is even a bit larger, so the improvement offered by our scheme is significant.

Charge-density differences around one carbon atom in C_2 are plotted in Fig. 1 for model densities showing three levels of accuracy. For present purposes, the difference density of a given model is the difference between the full self-consistent density generated from the one-electron

TABLE I. The binding energies (in eV) for three systems and seven model densities. The SCPW binding energies are given for cutoff l values [$L=l_{\max}(j)$] of 0, 1, 2, 3, and 4. The molecular orbital occupation numbers were constrained to be the same in all models for a given system.

System	FAF	SCAF	$L=0$	$L=1$	$L=2$	$L=3$	$L=4$
C_2	8.677	8.757	7.976	7.207	7.194	7.193	7.193
Fe_6Al_8	68.87	52.45	51.77	51.63	51.36	51.37	51.40
C_6H_6	76.78	75.04	68.90	68.37	68.12	68.03	68.04

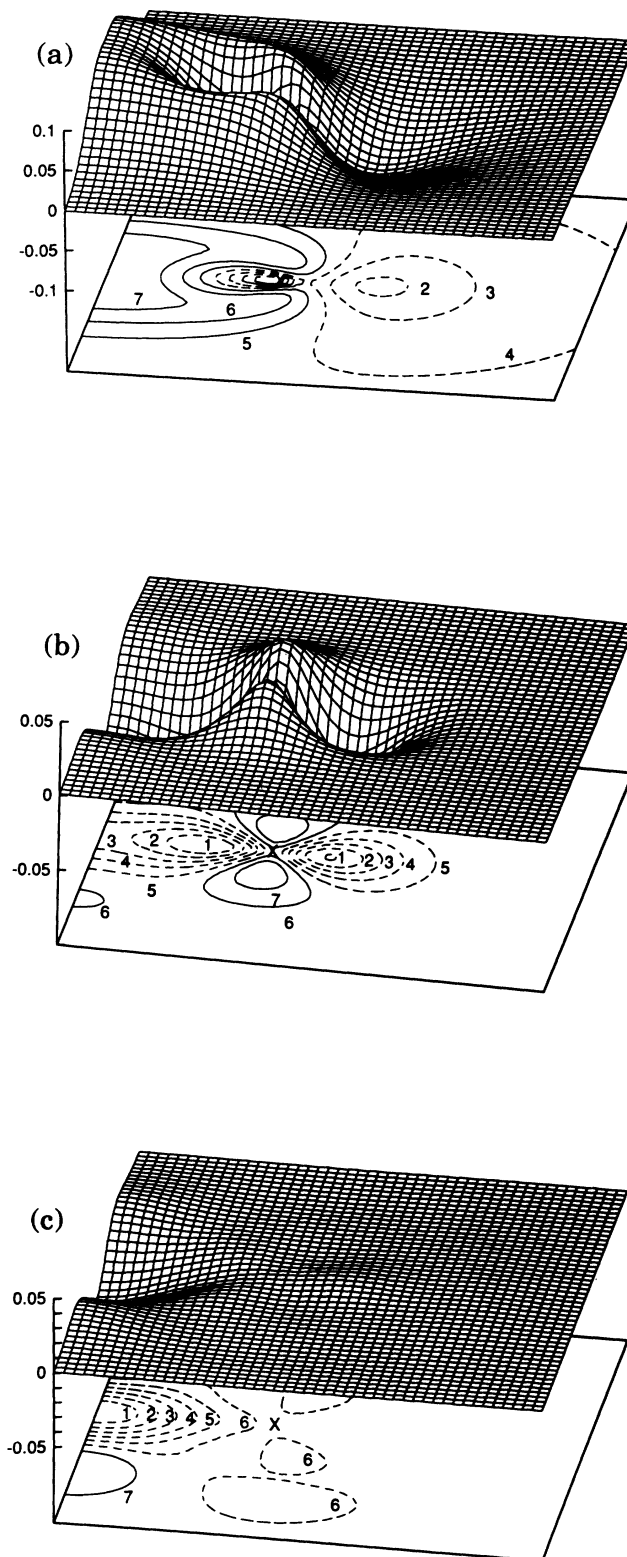


FIG. 1. Difference density expansions about one carbon atom in C_2 for SCPW model densities: (a) SCAF, (b) $l_{\max}(j)=1$, and (c) $l_{\max}(j)=2$. The symbol X marks the center of the carbon atom, and the vertical plane bisects the C-C bond (bond length = 2.36 bohr). For the contour plot in each panel, there are seven uniformly spaced contours with ranges of (a) -0.076 to 0.0679 , (b) -0.0549 to 0.0161 , and (c) -0.0202 to 0.00306 , in electrons/bohr³.

states in that model, $\rho(\mathbf{r})$, and the self-consistent model density $\bar{\rho}(\mathbf{r})$. Since both $\rho(\mathbf{r})$ and $\bar{\rho}(\mathbf{r})$ are normalized to the number of electrons, the difference density integrates to zero. In Fig. 1(a), the difference density is plotted for the SCAF model. As expected, restriction of the model density to a sum of spherically averaged atom densities leads to a significant error in the representation of the transfer of charge from the carbon atom to the region of the bond. The result of adding partial waves up to $l_{\max}(j)=1$ is apparent by comparing Figs. 1(a) and 1(b). The p -like component of the density, appearing as an "error density" in the SCAF model in Fig. 1(a), is replaced with a much smaller d -like error density distribution in Fig. 1(b) [note the change of scale between Figs. 1(a) and 1(b)]. Adding an additional partial wave [$l_{\max}(j)=2$] significantly reduces the error, leaving only the small difference density variations appearing in Fig. 1(c). As Table I shows, convergence in binding energies is rapid and essentially converged (within 0.1%) even with the density errors shown in Fig. 1(b).

B. Fe_6Al_8

Binding energies for different models and number of partial waves are also given for Fe_6Al_8 in Table I. This hypothetical cluster has O_h coordination with an Al atom at each corner of a cube and a Fe atom at the center of each face (a lattice fragment of the Cu_3Au structure). The calculations were carried out with a cube edge length (6.5336 a.u.) which is near the computed equilibrium bond length for this system. For calculations in the FAF model, the atomic valence configurations were chosen to be those of the experimental atomic ground states [i.e., $\text{Fe}(3d\uparrow^5 3d\downarrow^1 4s^2)$ and $\text{Al}(3s^2 3p\uparrow^1)$]. The SCAF calculation gives a self-consistent atomic population of $\text{Fe}(3d\uparrow^{3.95} 3d\downarrow^{2.16} 4s\uparrow^{1.04} 4s\downarrow^{1.17})$ and $\text{Al}(3s\uparrow^{0.82} 3s\downarrow^{0.90} 3p\uparrow^{0.56} 3p\downarrow^{0.48})$. The large error of the FAF calculation is explained on carrying out a SCAF calculation which shows a charge transfer of +0.24 electron/atom from the electropositive aluminum sites to the iron atoms. In order to verify that the improved binding energy of SCAF is due to this charge transfer, as opposed to a valence charge rearrangement *within* each atom (in particular, $3d$ spin flip on the Fe sites), a FAF calculation was performed using relaxed (but charge neutral) atom occupation numbers of $\text{Fe}(3d\uparrow^4 3d\downarrow^2 4s^2)$ and $\text{Al}(3s^2 3p\uparrow^{0.5} 3p\downarrow^{0.5})$. The computed binding energy of 87.4 eV is clearly in greater error than even the FAF results (see Table I) and thus indicates the importance of charge transfer in this system. Applying the SCPW method, including partial waves, only changes the binding energy from the SCAF result by 1.05 eV (2%). This suggests that the SCAF model alone is capable of describing the bonding in this system. As expected, the binding energy converges rapidly as partial waves are included in the calculation. An $l_{\max}(j)$ value of 2 on each site reduces the error in energy to 0.04 eV or 0.1%. Adding l values beyond 2 has only a marginal effect on the binding energy.

C. C_6H_6

Benzene was chosen as an application since the strong covalency in the bonding of this molecule presents a severe test of the various approximations discussed in the text. The binding energies of the benzene molecule appear in the third row of Table I. The C-C and C-H distances were 2.627 and 2.071 a.u., respectively, which are the calculated equilibrium separations for this molecule. In the FAF calculation, the atomic valence configurations were chosen to be $\text{C}(2s^2 2p\uparrow^1 2p\downarrow^1)$ and $\text{H}(1s\uparrow^{0.5} 1s\downarrow^{0.5})$. Indeed, the SCAF binding energy shows only a very modest improvement over the FAF approximation, which is itself in error by 8.7 eV (13%) relative to the SCPW results. Convergence of the SCPW binding energy with respect to $l_{\max}(j)$ is initially rapid. With $l_{\max}(j)=1$, the error in total binding energy is only 0.3 eV (0.4%), but for $l_{\max}(j)$ values beyond $l_{\max}(j)=1$, the convergence is noticeably slower. The $l_{\max}(j)$ value is a rate-determining factor for the computational time of a calculation, mainly since as $l_{\max}(j)$ increases, more angular grid points are required to carry out the partial-wave projections [Eq. (10)]. It could be argued, however, that convergence to better than 0.3 eV (0.4%) in total binding energy is probably not meaningful in light of the inaccuracies inherent in the local-density approximation.

D. Point convergence

Integration point convergence properties are a matter of practical concern in full-potential LDA calculations, and results for these three systems are summarized here. For the C_2 dimer with axial symmetry, the binding energy was converged to within 0.01 eV (0.1%) with $l_{\max}(j)=1$ and 325 points per atom. The Fe_6Al_8 cluster in O_h symmetry gave a binding energy converged to 0.03 eV (0.1%) with $l_{\max}(j)=2$ (on each site) and 1800 points per atom. Similarly, benzene (C_6H_6) with D_{6h} symmetry was converged to within 0.3 eV (0.5%) with $l_{\max}(j)=1$ (on each site), and 700 points per atom.

IV. DISCUSSION

The SCPW method is a logical and efficient development from the augmented Gaussian basis (AGB) and SCAF methods.^{19,22} Although developed independently, it shares several features with the recent DMol cluster method⁷ of Delley. First, both methods use a projection technique for generating a partial-wave charge-density expansion about each site. This is also an important component in the work of Becke.¹² Second, both methods use a Harris formalism for calculating total energies. In fact, it should be pointed out that Delley and his collaborators introduced a Harris-like approximation in rather early LDA cluster calculations.^{11,23} No doubt there are other points of commonality between the DMol and SCPW methods since they share some conceptual origins in the discrete-variational method of Ellis and Painter²⁴ and the self-consistent-charge method of Rosen *et al.*⁴

There are also a number of differences between DMol and SCPW: (1) DMol uses numerical basis functions instead of the Gaussian functions of the SCPW method.²⁵ The competing merits and disadvantages of Gaussian and numerical basis sets are well known.^{26,27} (2) The SCPW method uses symmetry to reduce the number of partial-wave components. (3) The sum of atom densities [Eq. (6)] is subtracted before the partial-wave projection in the SCPW method. The relative advantages of points (2) and (3) were discussed in the text.

In conclusion, we have shown how the SCAF method can be systematically improved by the addition of multi-center partial-wave components of the charge density, giving rise to the SCPW method. The method provides excellent flexibility for choosing the level of approxima-

tion used in a particular application (i.e., FAF, SCAF, or full SCPW). The computationally intensive step in each of these is the calculation of the numerical integrals, a task which is easily adapted to parallel processing. Although not covered here, the gradient interatomic forces^{8,28-31} can also be calculated, facilitating determination of equilibrium geometries.

ACKNOWLEDGMENTS

This work was supported by the Division of Materials Science, Office of Basic Energy Sciences, U.S. Department of Energy under Contract No. DE-AC05-84-OR21400 with Martin Marietta Energy Systems, Inc.

*Permanent address: Judson College, Elgin, IL 60123.

¹L. J. Sham, *Phys. Rev. B* **32**, 3876 (1985), and references therein; R. O. Jones and O. Gunnarsson, *Rev. Mod. Phys.* **61**, 689 (1989).

²E. J. Baerends, D. E. Ellis, and P. Ros, *Chem. Phys.* **2**, 41 (1973).

³H. Sambe and R. H. Felton, *J. Chem. Phys.* **61**, 3862 (1974).

⁴A. Rosen, D. E. Ellis, H. Adachi, and F. W. Averill, *J. Chem. Phys.* **65**, 3629 (1976).

⁵B. I. Dunlap, J. W. D. Connolly, and J. R. Sabin, *J. Chem. Phys.* **71**, 3396 (1979); **71**, 4993 (1979).

⁶B. Delley and D. E. Ellis, *J. Chem. Phys.* **76**, 1949 (1982).

⁷B. Delley, *J. Chem. Phys.* **92**, 508 (1990).

⁸F. W. Averill and G. S. Painter, *Phys. Rev. B* **41**, 10 344 (1990).

⁹J. Harris, *Phys. Rev. B* **31**, 1770 (1985).

¹⁰W. M. C. Foulkes and R. Haydock, *Phys. Rev. B* **39**, 12 520 (1989).

¹¹B. Delley, D. E. Ellis, A. J. Freeman, E. J. Baerends, and D. Post, *Phys. Rev. B* **27**, 2132 (1983).

¹²A. D. Becke and R. M. Dickson, *J. Chem. Phys.* **89**, 2993 (1988).

¹³S. F. Boys and P. Rajagopal, *Adv. Quantum Chem.* **2**, 1 (1965).

¹⁴A. D. Becke, *J. Chem. Phys.* **88**, 2547 (1988).

¹⁵J. Harris and G. S. Painter, *Phys. Rev. B* **22**, 2614 (1980).

¹⁶A. H. Stroud, *Approximate Calculation of Multiple Integrals* (Prentice-Hall, Englewood Cliffs, NJ, 1971).

¹⁷P. M. Boerrigter, G. te Velde, and E. J. Baerends, *Int. J. Quantum Chem.* **33**, 87 (1988).

¹⁸G. te Velde and E. J. Baerends, *J. Comput. Phys.* **99**, 84 (1992).

¹⁹F. W. Averill and G. S. Painter, *Phys. Rev. B* **39**, 8115 (1989).

²⁰S. H. Vosko, L. Wilk, and M. Nusair, *Can. J. Phys.* **58**, 1200 (1980).

²¹G. S. Painter, *Phys. Rev. B* **24**, 4284 (1981).

²²G. S. Painter and F. W. Averill, *Phys. Rev. B* **28**, 5536 (1983).

²³B. Delley (private communication).

²⁴D. E. Ellis and G. S. Painter, *Phys. Rev. B* **2**, 2887 (1970).

²⁵The use of Gaussian orbitals is not a requirement in the SCPW method, but simply reflects its development from the AGB method.

²⁶F. W. Averill and D. E. Ellis, *J. Chem. Phys.* **59**, 6412 (1973).

²⁷H. Chen, M. Krasowski, and G. Fitzgerald, *J. Chem. Phys.* **98**, 8710 (1993); J. Andzelm and E. Wimmer, *ibid.* **96**, 1280 (1992).

²⁸B. Delley, *J. Chem. Phys.* **94**, 7245 (1991).

²⁹R. Fournier, J. Andzelm, and D. R. Salahub, *J. Chem. Phys.* **90**, 6371 (1989).

³⁰R. Fournier, *J. Chem. Phys.* **92**, 5422 (1990).

³¹L. Verslius and T. Ziegler, *J. Chem. Phys.* **88**, 322 (1988).